

OPTIMUM DESIGN OF THE NICKEL CATALYSTS AND MECHANISTIC STUDY FOR CO₂ REFORMING WITH CH₄

Rong-Gang DING Zi-Feng YAN*

State Key Laboratory for Heavy Oil Processing, University of Petroleum,
Dongying 257062, P R China

ABSTRACT The possibility of optimizing the composition and the structures of the nickel catalysts and the pretreatment and reaction conditions for carbon dioxide reforming with methane is investigated. The optimum catalyst and the pretreatment and reaction conditions are determined employing the orthogonal and uniform design methods. The optimum nickel catalyst gives promising catalytic performance in terms of activity, selectivity and resistance to coke formation under the pretreatment and reaction conditions. The reaction behaviors and perfect performance of the optimum catalyst are extensively discussed. The properties of the surface carbon intermediates, which are produced by the decomposition of methane, using temperature-programmed desorption, temperature-programmed surface reaction, pulse reaction and on-line quadrupole mass spectroscopy techniques were also investigated. Carbidic C_α, carbonaceous C_β and carbidic clusters C_γ surface carbon species formed by decomposition of methane showed different surface mobility, thermal stability and reactivity. The possible reaction mechanism of carbon dioxide reforming with methane will also be postulated. Methane is firstly decomposed into hydrogen and different surface carbon species, then the adsorbed or gas phase CO₂ reacts with surface carbons to form CO.

KEYWORDS Optimum design, carbon dioxide reforming with methane, mechanism

1. INTRODUCTION

In recent years, catalytic reforming of carbon dioxide with methane to synthesis gas has been received new interest due to its environmental benefits and desired CO/H₂ ratio, than steam reforming for the production of hydrocarbons and oxygenated derivatives. Unfortunately, no commercial catalyst is yet available for the reforming of methane with carbon dioxide. Supported noble metals give promising catalytic performance in terms of activity, selectivity and resistance to coke formation.¹⁻³ Various nickel-based catalysts have been prepared and investigated in the past decades⁴⁻⁶ with different metal loadings, varieties and quantities of the promoters, and kinds of the supports. But there are few reports comparing the activity and stability of the catalysts with different compositions. No effective method to arrange the catalyst preparation and activity evaluation has yet been proposed. This paper aims at exploring possibility of optimizing the composition of the nickel catalysts and the pretreatment and reaction conditions employing orthogonal design and uniform design methods. There is a limiting amount of fundamental research concerning the reforming of methane with carbon dioxide over nickel-based catalysts. The present study also reports the characterization of the surface carbon intermediates produced in the reforming process and postulation of the reaction mechanism.

2. EXPERIMENTAL

2.1 Catalyst Preparation. A series of nickel-based catalysts were prepared with different supports, promoters and metal contents. La₂O₃, SiO₂, and two kinds of Al₂O₃ are selected as the catalyst supports. Nickel nitrate was loaded on the various supports by the incipient wetness impregnation method, then magnesium nitrate and cerous nitrate were added to the support by the same method. The nickel loading was set from 7.0% to 11.5% (wt%), while each promoter content was kept from 0 to 3% (wt%).

2.2 Catalytic Reaction. The reforming reaction was carried out in a continuous flow quartz fixed-bed reactor (i.d. 6mm) under atmospheric pressure and various reaction temperatures. The composition of reactants/products mixture was analyzed with an on-line SP-3420 gas chromatograph equipped with a TCD and a Porapak QS column.

2.3 Catalyst Characterization. The temperature-programmed experiments are conducted in the quartz fixed-bed reactor following the catalysts pretreatment. The catalysts are treated with oxygen for 30 min, then reduced with H₂ for 1 hr, finally cooled to room temperature and purged

* To whom correspondence should be addressed. E-mail: zfyang@hdpu.edu.cn
with He stream for 30 min.

The methane was pulsed continually on the pretreated catalysts using high purity helium as carrier gas at 973 K. Subsequently, a 20 ml/min flow of hydrogen or mixed gas of CO₂/He (1:10) was introduced to flush the reactor continuously to take away the gaseous and physically adsorbed mixture after cooling to room temperature. Then the TPSR was initiated in the hydrogen or mixed gas of CO₂/He at a heating rate of 20 K/min. When the temperature was

increased to 1000 K, the carrier gas was switched again, then H₂ and O₂ were pulsed respectively into the micro-reactor under high temperature. The desorbed products from the metal surface along with the temperature-programmed process were simultaneously detected by on-line ion trap detector (ITD).

TPD experiments were conducted at a constant heating rate (10 K/min), using ultra high purity helium as carrier gas, at a flow rate of 40 ml/min. The reforming reaction was carried out in situ at certain temperature and then the reactor was quickly cooled to room temperature. After purging with He for 30 min, the temperature programming was initiated and the analysis of the desorbed gases was performed with the on-line ITD.

In the TPD process, the helium gas was dried with Mg(ClO₄)₂ and deoxygenated with 402 deoxygenating reagent. The residual oxygen that might flow over the catalyst was removed by using liquid nitrogen cold trap before flowing into the reactor. Leak tests on the reaction system were also strictly performed to exclude the possibility of the oxidation of surface carbonaceous species.

3. RESULTS AND DISCUSSION

3.1 Catalyst Optimization. A series of nickel-based catalysts, with various supports, promoters and metal loadings, were prepared by incipient wetness impregnation method according to a certain orthogonal design table. The L₂₅ (4⁵) orthogonal table is employed to arrange the preparation of catalysts and investigate the interaction between metal and support. In this table, the support-metal strong interaction was considered an important factor. The orthogonal design experimental results for the reforming catalyst are shown as Table 1.

The optimum pretreatment and reaction conditions were determined by a large number of experiments employing the uniform method. Its characteristic and application in the catalytic scientific community will be discussed elsewhere. Catalytic performance tests for all catalysts were carried out under the optimum pretreatment and reaction conditions.

The total molar concentration of CO and H₂ (dry base) is used to evaluate the performance of catalysts. It can be seen that the effect of the factors on the performance of the catalyst is as follows: support > Ni metal loading > MgO addition > CeO₂ addition > interaction between metal and support. It is found that the support shows more influence than metal loading on the performance of catalysts within appropriate metal loading range. It gives evidence that understanding of the nature of support and selection of support may be very important for improving the catalyst.

The weak interaction between metal and support may be attributed to the preparation conditions of the catalysts. In the meantime, MgO and CeO₂ promoter exhibit approximate effect on the activity of catalysts. It can be seen from Table 1 that the OD-5 catalyst is the best reforming catalyst in this experiment. Indeed, it provides 91.3% and 86.9% conversions of CO₂ and CH₄, 86.8% and 89.1% yields of H₂ and CO at 973K, respectively. According to the experimental results, it is deduced that the optimum catalyst constitutes can be described as follows: 8.5 wt% Ni loading supported on Al₂O₃-1 with 3 wt% MgO and 3 wt % CeO₂ added.

The catalyst activity exhibited in Table 1 is the integrative result of the collective effect of metal loading, support, promoter, and interaction between support and metal. It is very difficult to simply compare one catalyst with another in terms of certain factor's influence on the performance of catalyst when the catalyst are prepared and tested according to a orthogonal design method. The orthogonal design considers all factors as an indivisible one and arranges them efficiently to simplify the catalyst screening. For the heavy and complicated catalyst screening, the orthogonal design method may be a desired choice. As a matter of fact, the orthogonal design method has applied to many scientific fields. But to our knowledge less applications of the orthogonal design in catalyst preparation and screening have been reported. In this work, we try to make use of this method to optimize the catalyst and simplify the catalyst screening process. It is convinced of the rapid development of the catalyst orthogonal screening technique in near future.

3.2 Catalyst Characterization.

H₂ TPSR of the catalyst. A great effort was made to detect adsorbed carbonaceous CH_{x(ad)} fragments formed in the decomposition of methane by means of sensitive *in-situ* FT-IR spectroscopy. However, no adsorption bands attributable to any vibration modes of carbonaceous CH_{x(ad)} species were identified either by *in-situ* measurements or after a sudden cooling of the sample in a continuous methane flow at 700 K. This means that all the above carbonaceous CH_{x(ad)} species react or decompose too quickly at high temperature, or their surface concentrations are below the detection limit.

However, the presence of surface carbonaceous CH_{x(ad)} species was well manifested by its reaction with hydrogen. After flushing the reactor with pure helium flow (following methane decomposition at a certain temperature) and switching to a hydrogen flow, the hydrogenation of the surface carbonaceous CH_{x(ad)} species was investigated by TPSR technique. Figure 1 showed that the decomposition of methane could result in the formation of at least three kinds of surface

carbon species on supported nickel catalyst. Generally, the carbon deposition is comprised of various forms of carbon species which are different in terms of reactivity. The distribution and features of these carbonaceous species depend sensitively on the nature of transition metals and the conditions of methane adsorption. These carbonaceous species can be described as: completely dehydrogenated carbidic C_α type, partially dehydrogenated CH_x ($1 \leq x \leq 3$) species, namely C_β type, and carbidic clusters C_γ type formed by the agglomeration and conversion of C_α and C_β species under certain conditions.

A fraction of the surface carbon species, which might be assigned to carbidic C_α (~461 K), was mainly hydrogenated to methane even below 500 K. Simultaneously, a trace of ethane was also produced in addition to methane. It shows that carbidic C_α species is rather active and thermally unstable on nickel surface. The significant amount of surface carbon species was hydrogenated to methane below 600 K and was assigned to partially dehydrogenated C_β (~583 K) species. The majority of the surface carbon was hydrogenated above 800 K and was attributed to carbidic clusters C_γ (~823 K). The formation of less active C_γ species causes the catalyst deactivation.⁸ It also indicated that the formation of three kinds of surface carbon species with different structures and properties largely depend on the exposure temperature and duration to methane. When the nickel catalyst was exposed to methane above 723 K, the carbidic C_α species was not detected, and a significant amount of C_β was transformed into the carbidic clusters C_γ . It shows that the carbidic clusters C_γ species might be the precursor of the surface carbon deposition, which may be produced by the interactions between C_α and C_β species and between C_α and C_β themselves.

TPD of used catalyst. The TPD profiles of used Ni/Al_2O_3 catalyst after 8 h of reaction were shown in Figure 2. Compared with CO -TPD profiles over the fresh Ni/Al_2O_3 catalyst, on which two respective CO_2 desorption peaks appear, an additional intense CO_2 peak at ca. 910 K was observed on used catalyst.

The two CO_2 desorption peaks appear on both the TPD of used catalyst and the CO -TPD profiles over the fresh catalyst at ca. 410 K and 570 K. They seem to correspond to the desorbed CO_2 in the form of weakly chemisorbed on different sites on both catalysts. It is interesting to note that a large quantity of CO and CO_2 desorbed at approximately the same temperature from at ca. 800 K, but the increase of CO obviously lagged behind. This indicates that CO might be the secondary product rather than primary one. The interaction of surface carbon with gaseous CO_2 would result in the formation of CO . The obvious hysteresis effect of CO peak with respect to CO_2 peak and the continuous increase of intensity of CO peak are noteworthy. This could be manifested by the mobility of the surface carbon species and the reactivity of the oxygen species on the nickel catalyst. The mobile surface carbon species can attack the neighboring oxygen adatoms and surface oxygen species to form CO or CO_2 . It is also possible that the CO_2 desorbed from the catalyst re-adsorbed and then reacted with surface carbonaceous species to produce CO . The carbon species originally produced by methane are believed to be atomic or carbidic carbon. It is known to be a very active and important intermediate in the CO_2 reforming of methane. The interaction between the adsorbed or gaseous CO_2 and surface carbon species can result in the formation of CO . Based on this consideration, the possible reaction processes of CO_2 reforming of methane can be inferred as follows: methane is firstly decomposed into hydrogen and different surface carbon species, then the adsorbed or gas phase CO_2 reacts with surface carbons to form CO .

CO_2 TPSR and pulse reaction of H_2 and O_2 . Firstly, TPSR was performed in the mixed gas of CO_2/He (1:10) following CH_4 pulses over reduced Ni/Al_2O_3 catalyst (Figure 3), then the H_2 or O_2 pulse was introduced into the reactor (Figure 4). A fraction of CO_2 adsorbs on the catalyst at about 300 K and desorbs from 600 K in the CO_2/He flow. The equilibrium between the surfaced adsorbed and gaseous CO_2 is responsible for the high CO_2 desorption temperature than that in He flow. The formation and desorption of CO can be observed while surfaced CO_2 begins to desorb greatly. The consumption of CO_2 and formation of CO reach the maximum at elevated temperature of 740 K. The CO_2 TPSR on the Ni catalyst may give a deduction of the pathway of CO_2 : firstly adsorbs on the surface of the catalyst, then reacted with neighboring surface carbonaceous species to form CO . This is similar to the inference from the TPD experiment of the used catalyst as Figure 2 showed.

The formation of CH_4 is not detected in the H_2 pulse reaction following CO_2 TPSR at 973 K. It shows that the surface carbonaceous species which can react with CO_2 have used up. This type of surface carbonaceous species is active and can react with not only CO_2 but also with H_2 . At the same time, other inertial carbonaceous species may exist on the surface of the catalyst. The O_2 pulse reaction is continually carried out following the CO_2 TPSR and H_2 pulse reaction in order to verify the existence of other carbonaceous species. The appearance of CO_2 corresponding to the O_2 pulses is good evidence for the existence of the other carbonaceous species, which is difficult to react with H_2 or CO_2 . The catalyst deactivation may result from the deposited carbon species, which does not react with H_2 or CO_2 but react with O_2 at high temperature.

Figure 1 becomes conscious of the emergence of at least three kinds surface carbonaceous species at lower temperature. When the catalyst was exposed to methane at 973 K, the carbidic C_α species was completely converted into C_β or C_γ species. The partially dehydrogenated C_β

species can react with H₂ or CO₂ to form CH₄ or CO, but the less active carbidic clusters C_γ species can not react with H₂ or CO₂ even at very high temperature. The H₂ and CO₂ TPSR and pulse reaction provide the mutual verification of the existence and property of the surface carbonaceous species. The further investigation towards the properties of the surface carbon species is the key to suppressing the catalyst deactivation and elucidating the mechanism of the reforming reaction.

4. CONCLUSIONS

- (1) The orthogonal design method can simplify the catalyst screening process and evaluate the principal effect and its degree of influence on the performance of the catalyst.
- (2) Carbidic C_α, carbonaceous C_β and carbidic clusters C_γ surface carbon species formed by decomposition of methane showed different surface mobility, thermal stability and reactivity. C_α and C_β species are active and the carbidic clusters C_γ species might be the precursor of the surface carbon deposition.
- (3) The possible reaction processes may be as follows: methane is firstly decomposed into hydrogen and different surface carbon species, then the adsorbed or gas phase CO₂ reacts with surface carbons to form CO.

ACKNOWLEDGEMENTS

Financial supports by the Young Scientists Award Foundation of Shandong Province and Young Scientists Innovation Foundation of China National Petroleum Corporation are gratefully acknowledged.

REFERENCES

- (1) Solymosi, F.; Kustan, G.; Erdohelyi, A. *Catal. Lett.* **1991**, *11*, 144.
- (2) Vennon, P. D. F.; Green, H. M. *Catal. Today* **1992**, *13*, 417.
- (3) Richardson, J.T.; Paripatyadar, S.A. *Appl. Catal.* **1990**, *61*, 293.
- (4) Gadalla, A.M.; Bower, B. *Chem. Eng. Sci.* **1988**, *43*, 3049.
- (5) Yamazaki, O.; Nozaki, T.; Omata, K.; Fujimoto, K. *Chem. Lett.* **1992**, 1953.
- (6) Chen, Y. G.; Yamazaki, O.; Tomishige K.; Fujimoto, K. *Catal. Lett.* **1996**, *39*, 92.
- (7) Wang, S. B.; Lu, G. Q. *Ind. Eng. Chem. Res.* **1997**, *36*, 5103.
- (8) Zhang, Z.; Verykois, X. E. *Catal. Today* **1994**, *21*, 589.

Table 1 Orthogonal design experimental results
(T = 973 K, P = 1atm, CH₄/CO₂ = 1.05)

factor number	A Ni (wt%)	B support	A MgO (wt%)	B CeO ₂ (wt%)	C	D	(CO+H ₂) concn. (dry mol%)	CH ₄ conv. (%)	CO ₂ Conv. (%)	H ₂ yield (%)	CO yield (%)
1	7.0	Al ₂ O ₃ -1	1	0	0		71.2	74.6	79.7	74.0	77.2
2	7.0	Al ₂ O ₃ -2	2	1	1		75.8	79.5	85.7	784	82.6
3	7.0	La ₂ O ₃	3	2	2		46.5	48.7	54.6	47.0	51.7
4	7.0	SiO ₂	4	3	3		68.1	69.7	77.0	67.9	73.4
5	8.5	Al ₂ O ₃ -1	2	2	3		84.8	86.9	91.3	86.8	89.1
6	8.5	Al ₂ O ₃ -2	1	3	2		79.2	81.9	89.3	80.3	85.6
7	8.5	La ₂ O ₃	4	0	1		54.3	57.7	68.7	53.8	63.2
8	8.5	SiO ₂	3	1	0		61.4	64.3	71.5	62.4	67.9
9	10	Al ₂ O ₃ -1	3	3	1		77.3	79.9	86.8	78.5	83.4
10	10	Al ₂ O ₃ -2	4	2	0		66.5	68.7	75.1	67.3	71.9
11	10	La ₂ O ₃	1	1	3		52.4	54.0	61.1	51.9	57.8
12	10	SiO ₂	2	0	2		56.3	58.4	61.6	58.3	60.0
13	11.5	Al ₂ O ₃ -1	4	1	2		62.3	64.6	73.4	62.0	69.0
14	11.5	Al ₂ O ₃ -2	3	0	3		59.3	62.0	69.1	60.0	65.6
15	11.5	La ₂ O ₃	2	3	0		48.9	51.2	59.2	48.6	55.3
16	11.5	SiO ₂	1	2	1		49.6	51.6	59.3	49.2	55.5
R			14.9	23.4	3.7	8.1	7.1				
prior level		A ₂	B ₁	(A B) ₂	C ₄	D ₄					
factor order		2	1	5	3	4					

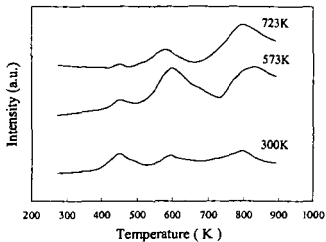


Figure 1. TPSR spectra of CH_4 in H_2 flow on fresh 8wt% $\text{Ni}/\text{Al}_2\text{O}_3$ at different adsorption temperatures

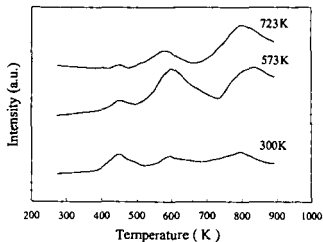


Figure 2. TPD profile over the used 8wt% nickel catalyst supported on alumina

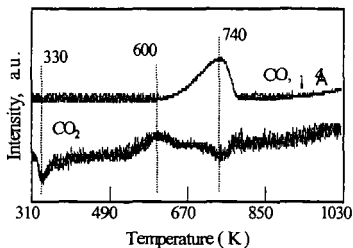


Figure 3. TPSR in CO_2/He (1:10) stream following CH_4 pulse at 973K over reduced $\text{Ni}/\text{Al}_2\text{O}_3$ catalyst.

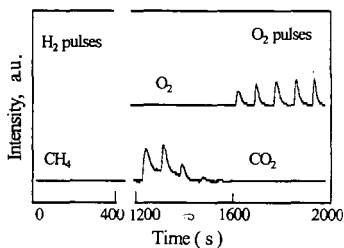


Figure 4. H_2 and O_2 pulses patterns at 973K following CO_2 TPSR over $\text{Ni}/\text{Al}_2\text{O}_3$ catalyst.